

Signal Reconstruction from Two Close Fractional Fourier Power Spectra

Tatiana Alieva, Martin J. Bastiaans, and Ljubiša Stanković

Abstract—Based on the definition of the instantaneous frequency (signal phase derivative) as a local moment of the Wigner distribution, we derive the relationship between the instantaneous frequency and the derivative of the squared modulus of the fractional Fourier transform (fractional Fourier transform power spectrum) with respect to the angle parameter. We show that the angle derivative of the fractional power spectrum can be found from the knowledge of two close fractional power spectra. It permits us to find the instantaneous frequency and to solve the phase retrieval problem up to a constant phase term, if only two close fractional power spectra are known. The proposed technique is noniterative and noninterferometric. Efficiency of the method is demonstrated on several examples including monocomponent, multicomponent, and noisy signals. It is shown that the proposed method works well for signal-to-noise ratios (SNRs) higher than about 3 dB. The appropriate angular difference of the fractional power spectra used for phase retrieval depends on the complexity of the signal and can usually reach several degrees.

Other applications of the angular derivative of the fractional power spectra for signal analysis are discussed briefly.

The proposed technique can be applied for phase retrieval in optics, where only the fractional power spectra associated with intensity distributions can be easily measured.

I. INTRODUCTION

Phase retrieval and instantaneous frequency estimation from the distributions associated with the instantaneous power of the signal, its Fourier power spectrum, or, more generally, its fractional power spectra, are important problems in signal processing, radio location, optics, quantum mechanics, etc. In spite of the existence of several successful iterative algorithms for phase reconstruction from the squared modulus of the signal and its power spectrum, or its Fresnel spectrum, that were

proposed recently [1]-[4], the development of noniterative procedures remains an attractive research topic.

Fractional power spectra, which are the squared moduli of the fractional Fourier transform (FT) [5], are now a popular tool in optics and signal processing [5]-[13]. As it is known, they are equal to the projections of the Wigner distribution of the signal under consideration [13], [14]. Thus, by using a tomographic approach and the inverse Radon transform, the Wigner distribution – and therefore the signal itself, up to a constant phase term – can be reconstructed if all its projections are known [6], [9]. The method is based on the rotation in the time-frequency plane of the Wigner distribution under fractional FT. It demands the measurements of the fractional FT spectra in the wide angular region $[0, \pi)$, which is sometimes impossible or very cost consuming [6].

A different approach for phase retrieval, based on the so-called transport-of-intensity equation in optics, was proposed by Teague [15] and then further developed in [16]-[18]. It was shown that the longitudinal derivative of the Fresnel spectrum is proportional to the transversal derivative of the product of the instantaneous power and the instantaneous frequency of the signal.

In this paper, we show that a relationship similar to the transport-of-intensity equation for Fresnel diffraction also holds for the fractional FT system. We derive that the instantaneous frequency, or the first derivative of the signal's phase, at any fractional domain is determined by the convolution of the angular derivative of the corresponding fractional power spectrum and the signum function. Based on this, we propose a new method for the reconstruction of the signal's phase from only two close fractional FT spectra,

i.e., only two Wigner distribution projections. Some preliminary results on this topic were published in [20], [21]. This approach significantly reduces the need for projections measurements and calculations. Moreover, it is direct and does not use iterative procedures. Note that the Gerchberg-Saxton algorithm applied in the fractional Fourier domain for phase retrieval from two fractional FT power spectra for angles α and $\alpha + \Delta\alpha$ becomes unstable and does not converge if $\Delta\alpha < 15^\circ$ [1], while our method works especially for small $\Delta\alpha$.

We show that this technique can also be applied for signal reconstruction from certain projections of other time-frequency distributions from the Cohen class [19]. The application of angular derivative of the fractional power spectrum for signal/image processing is discussed.

The efficiency of the proposed method is illustrated on several examples. In particular, the reconstruction of monocomponent and multicomponent PM signals from several pairs of close fractional FT power spectra is considered. The influence of noise and angle difference to the estimation of angular derivative of the fractional power spectrum, and to the reconstruction quality is investigated. Note that the noise robustness was not considered in [1]-[4]. These papers were devoted to the recursive algorithms for phase retrieval from the fractional FT power spectra. Signal reconstruction from fractional power spectra taken in the fractional Fourier domain, where the instantaneous power of a signal significantly changes, is considered. We discuss the reconstruction of the signal with zero-amplitude region.

The paper is organized as follows. In Section II, we present a review of the definition of the fractional FT, as well as the relationship between the fractional FT power spectra and the ambiguity function of a signal. In Section III the connection between the instantaneous frequency in a fractional domain and the angular derivative of the fractional FT power spectra is established. Similar relationships between the projections of Cohen's class distributions and the instantaneous frequency are briefly discussed. Some practical issues with respect to phase retrieval from two close frac-

tional FT power spectra are discussed in Section IV. Useful relationships for signal/image analysis, including the derivatives of fractional spectra, are given in Section V. In Section VI we discuss the discrete version of the proposed phase retrieval method. Section VII is devoted to the demonstration of its efficiency on several examples. The advantages of the new algorithm and its possible applications are discussed in the Conclusions.

II. FRACTIONAL POWER SPECTRA AND AMBIGUITY FUNCTION

The fractional FT of a function $x(t)$ can be written in the form [5]

$$R^\alpha[x(t)](u) = X_\alpha(u) = \int_{-\infty}^{\infty} K(\alpha, t, u)x(t)dt, \quad (1)$$

where the kernel $K(\alpha, t, u)$, which is a generalized function, is given by

$$K(\alpha, t, u) = \frac{e^{j\frac{1}{2}\alpha}}{\sqrt{j \sin \alpha}} e^{j\pi \frac{(t^2+u^2) \cos \alpha - 2ut}{\sin \alpha}}. \quad (2)$$

Thus, for $\alpha = 0$ and $\alpha = \pi$ the kernel $K(\alpha, t, u)$ reduces to the Dirac delta functions $\delta(x - u)$ and $\delta(x + u)$, respectively; therefore $X_0(u) = x(u)$ and $X_\pi(u) = x(-u)$. The fractional FT can be considered as a generalization of the ordinary FT: For the parameter values $\alpha = \frac{1}{2}\pi$ and $\alpha = -\frac{1}{2}\pi$, the transforms $X_{\pi/2}(u)$ and $X_{-\pi/2}(u)$ correspond to the ordinary forward and inverse FT, respectively. The fractional FT is additive in the parameter α and periodic with a period 2π . Due to the fact that the fractional FT corresponds to a rotation of the Wigner distribution [19]

$$W_x(t, f) = \int_{-\infty}^{\infty} x(t + \frac{1}{2}\tau)x^*(t - \frac{1}{2}\tau)e^{-j2\pi f\tau} d\tau,$$

and the ambiguity function

$$A_x(\tau, \nu) = \int_{-\infty}^{\infty} x(t + \frac{1}{2}\tau)x^*(t - \frac{1}{2}\tau)e^{-j2\pi\nu\tau} dt,$$

of the function $x(t)$, the parameter α can be interpreted as a rotation angle in the phase plane.

It is well known that the fractional power spectra $|X_\alpha(u)|^2$, i.e., the squared moduli of the fractional FT, are equal to the projections of the Wigner distribution $W_x(t, f)$ of the signal $x(t)$

$$\begin{aligned} |X_\alpha(u)|^2 &= \\ & \int_{-\infty}^{\infty} \int_{-\infty}^{\infty} W_x(t, f) \delta(t \cos \alpha + f \sin \alpha - u) df dt \\ &= \int_{-\infty}^{\infty} W_x(u \cos \alpha - f \sin \alpha, u \sin \alpha + f \cos \alpha) df. \end{aligned} \quad (3)$$

The set of fractional power spectra in the angular region $[0, \pi)$ is also called the Radon-Wigner transform. The implementation of the inverse Radon transform permits the reconstruction of the Wigner distribution from this set.

Since the ambiguity function $A_x(\tau, \nu)$ is the two-dimensional (2-D) FT of the Wigner distribution $W_x(t, f)$, the values of the ambiguity function along the line defined by α are – according to the Radon transform properties – equal to the FT of the Wigner distribution projection for the same α [7], [9]:

$$\begin{aligned} A_x(R \sin \alpha, -R \cos \alpha) &= \\ & \int_{-\infty}^{\infty} |X_\alpha(u)|^2 \exp(j2\pi Ru) du. \end{aligned} \quad (4)$$

We can also say that the fractional power spectrum $|X_\alpha(u)|^2$ is the FT with respect to the radius variable R of the ambiguity function represented in polar coordinates.

III. WIGNER DISTRIBUTION PROJECTIONS AND INSTANTANEOUS FREQUENCIES

In this section we, derive that the well-known expression for the instantaneous frequency $f_0(t)$ at the time moment t [19]

$$\begin{aligned} f_0(t) &= \frac{\int_{-\infty}^{\infty} f W_x(t, f) df}{\int_{-\infty}^{\infty} W_x(t, f) df} \\ &= \frac{1}{2\pi j} \frac{1}{|x(t)|^2} \int_{-\infty}^{\infty} \frac{\partial A_x(\tau, \nu)}{\partial \tau} \Big|_{\tau=0} e^{j2\pi t \nu} d\nu \end{aligned} \quad (5)$$

can be written in terms of the fractional power spectra. Indeed, using the relationship [20]

$$\begin{aligned} \frac{\partial A_x(\tau, \nu)}{\partial \tau} \Big|_{\tau=0} &= \\ & -\frac{1}{\nu} \int_{-\infty}^{\infty} \frac{\partial |X_\alpha(u)|^2}{\partial \alpha} \Big|_{\alpha=0} e^{-j2\pi \nu u} du, \end{aligned} \quad (6)$$

and taking into account that $f_0(t)$ assumes real values, we get

$$\begin{aligned} f_0(t) &= \frac{-1}{2\pi |X_0(t)|^2} \int_{-\infty}^{\infty} \int_{-\infty}^{\infty} \frac{\partial |X_\alpha(u)|^2}{\partial \alpha} \Big|_{\alpha=0} \\ & \times \frac{\sin(2\pi \nu(t-u))}{\nu} du d\nu. \end{aligned}$$

Supposing that the derivative of the fractional power spectra is a continuous function of u , we change the order of integration. Then we obtain that

$$\begin{aligned} f_0(t) &= \frac{-1}{2 |X_0(t)|^2} \\ & \times \int_{-\infty}^{\infty} \frac{\partial |X_\alpha(u)|^2}{\partial \alpha} \Big|_{\alpha=0} \operatorname{sgn}(t-u) du, \end{aligned} \quad (7)$$

where $\operatorname{sgn}(t)$ is the signum function:

$$\operatorname{sgn}(t) = \frac{2}{\pi} \int_0^{\infty} \frac{\sin(\nu t)}{\nu} d\nu = \begin{cases} 1 & \text{for } t > 0, \\ 0 & \text{for } t = 0, \\ -1 & \text{for } t < 0. \end{cases} \quad (8)$$

We thus get for the signal $x(t) = |X_0(t)| \times \exp[j\varphi_0(t)]$, that its phase derivative $\varphi'_0(t) = d\varphi_0(t)/dt = 2\pi f_0(t)$ is determined by the intensity $|X_0(t)|^2$ and the convolution of the signum function with the angular derivative of the fractional power spectrum $\partial |X_\alpha(u)|^2 / \partial \alpha$ at the angle $\alpha = 0$.

Note that for a real-valued signal, the angular derivative of its fractional power spectra equals zero for $\alpha = 0$. This is in accordance with the fact that the fractional FT of a real-valued signal $x(t)$ satisfies the symmetry relation $X_{-\alpha}(u) = X_\alpha^*(u)$, and thus $|X_{-\alpha}(u)|^2 = |X_\alpha(u)|^2$.

Because of the properties of the fractional FT, (7) can easily be generalized for an arbitrary angle $\alpha \neq 0$ [20]

$$f_\beta(r) = \frac{-1}{2 |X_\beta(r)|^2} \times \int_{-\infty}^{\infty} \frac{\partial |X_\alpha(u)|^2}{\partial \alpha} \Big|_{\alpha=\beta} \text{sgn}(r-u) du, \quad (9)$$

where $|X_\beta(r)|^2$ and $f_\beta(r)$ are the instantaneous power and the instantaneous frequency of the signal in the fractional FT domain corresponding to the angle β . We notice that in general the reconstruction of the instantaneous frequency has sense if the amplitude is non zero. Therefore, in general, we suppose that $|X_\beta(r)|^2$ does not take zero values. Nevertheless, as we will show in Section VII (Example 2) the instantaneous frequency can be successfully reconstructed in the intervals limited by the zero-crossings of the amplitude.

The instantaneous frequency of the signal $x(r) = X_0(r)$ can also be found from close projections $p_\alpha^c(u)$ of other time-frequency distributions from the Cohen class [19] $C_x(t, f)$ satisfying the generalized marginal property. A Cohen class distribution is a 2-D FT of the generalized ambiguity function $A_x^c(\tau, \nu) = A_x(\tau, \nu)c(\tau, \nu)$, where the choice of the function $c(\tau, \nu)$ depends on the particular application. According to the Radon transform properties, we then get [cf. (4)]

$$A_x(R \sin \alpha, -R \cos \alpha) c(R \sin \alpha, -R \cos \alpha) = \int_{-\infty}^{\infty} p_\alpha^c(u) \exp(j2\pi Ru) du, \quad (10)$$

where

$$p_\alpha^c(u) = \int_{-\infty}^{\infty} \int_{-\infty}^{\infty} C_x(t, f) \delta(t \cos \alpha + f \sin \alpha - u) df dt,$$

cf. (3). For distributions satisfying the generalized marginal property $c(R \sin \beta, -R \cos \beta) = 1$ for a certain angle β , we get $p_\beta^c(u) =$

$|X_\beta(u)|^2$. Hence, for these Cohen class distributions, we can expect that [cf. (9)]

$$f_\beta(r) = \frac{-1}{2 p_\beta^c(r)} \int_{-\infty}^{\infty} \frac{\partial p_\alpha^c(u)}{\partial \alpha} \Big|_{\alpha=\beta} \text{sgn}(r-u) du. \quad (11)$$

A special and important member of the Cohen class is the *pseudo* Wigner distribution, which, as well as the Wigner distribution itself, is often used in numerical implementations. For this distribution, we have $c(\tau, \nu) = w(\tau)$, where $w(\tau) = w^*(-\tau)$ is an appropriately chosen window function with $w(0) = 1$. For $\beta \rightarrow 0$ we get $c(R \sin \beta, -R \cos \beta) \rightarrow c(0, -R) = w(0) = 1$. Therefore, this lag window does not significantly influence the quality of the signal reconstruction as long as β is small.

IV. PHASE RETRIEVAL FROM TWO CLOSE FRACTIONAL FT POWER SPECTRA

In general, the complex-valued fractional FT $X_\beta(r) = |X_\beta(r)| \exp[j\varphi_\beta(r)]$, and, in particular, the signal $x(t) = X_0(t)$, can be completely reconstructed (except for a constant phase shift) from its intensity distribution $|X_\beta(r)|^2$ and its instantaneous frequency $f_\beta(r)$. Since $d\varphi_\beta(r)/dt = 2\pi f_\beta(r)$, the phase $\varphi_\beta(r) = 2\pi \int_C^r f_\beta(\rho) d\rho$ can be reconstructed up to a constant term. Constant C produces a phase uncertainty. Since the instantaneous frequency is determined by the angular derivative of the fractional power spectra (see (7) and (9)), this implies that only two fractional power spectra for close angles suffice to solve the signal retrieval problem, up to the constant phase term. Indeed, as it follows from the Taylor expansion of the fractional power spectrum in the region where the linear approximation with respect to the parameter α is valid, we can represent its angular derivative as

$$\frac{\partial |X_\alpha(u)|^2}{\partial \alpha} \Big|_{\alpha=\beta} \approx \lim_{\alpha \rightarrow 0} \frac{|X_{\beta+\alpha}(u)|^2 - |X_{\beta-\alpha}(u)|^2}{2\alpha}. \quad (12)$$

The accuracy of this approximation is $O(\alpha^2 \partial^3 |X_\alpha(u)|^2 / \partial \alpha^3 |_{\alpha=\beta})$. Moreover, from

the knowledge of two fractional power spectra $|X_{\beta+\alpha}(u)|^2$ and $|X_{\beta-\alpha}(u)|^2$, the fractional power spectrum $|X_{\beta}(u)|^2$ can be found as

$$|X_{\beta}(u)|^2 = \frac{1}{2} \left(|X_{\beta+\alpha}(u)|^2 + |X_{\beta-\alpha}(u)|^2 \right) + O \left(\alpha^2 \partial^2 |X_{\alpha}(u)|^2 / \partial \alpha^2 \Big|_{\alpha=\beta} \right). \quad (13)$$

Because $x(t)$ is related to $X_{\beta}(r)$ through the inverse fractional FT, we can conclude that the signal phase can be reconstructed up to a constant term – in a noniterative way – from any two fractional power spectra taken for close angles. The choice of the appropriate angular difference α depends on the complexity of the signal.

Beside the general importance of the noniterative and noninterferometric phase reconstruction from the intensity information only, this technique can be applied to the filtering operation. It has been shown that, in some cases, filtering is more effective in the fractional FT domain than in the Fourier domain [23]. Thus, for example, filtering of the linear-PM signal $\exp(j\pi ct^2)$ can be successfully performed in the fractional domain for which the angle parameter α satisfies the condition $\cos \alpha + c \sin \alpha = 0$ [5]; see Case 1 of Section V. Another example [23] is related to the signal-noise separation in a certain fractional domain.

Often, for example in optics, only information about the fractional FT *spectra* is available. Before applying the proposed signal reconstruction technique, an appropriate filtering (modification) of the corresponding fractional FT spectra can be carried out. Certainly, after this operation, the fractional FT spectra have to remain positive valued. The simplest modifications of two close fractional FT spectra are related to the elimination of the undesirable peaks associated with concentration of linear-PM components or of noise-only regions.

V. SIGNAL ANALYSIS AND FRACTIONAL FT POWER SPECTRA DERIVATIVES

In this section, we briefly discuss other problems that can be solved from the analysis of the

derivatives of the fractional FT power spectrum. This topic becomes especially important if the signal itself is not known, and only its close fractional FT power spectra (Wigner distribution projections) are available. Such a situation occurs in optics, for example, where only intensity distributions related to the fractional power spectra can easily be measured.

As we have seen, the instantaneous frequency (or normalized first derivative of the phase) of a signal in the fractional β domain is related to the angular derivative of the fractional power spectrum by (9). Then, by using the relationship $(d/dr) \operatorname{sgn}(r) = 2\delta(r)$, we obtain the expression for the second derivative of the phase

$$\frac{d^2 \varphi_{\beta}(r)}{dr^2} = -\frac{2}{|X_{\beta}(r)|} \frac{\partial |X_{\beta}(r)|}{\partial r} \frac{d\varphi_{\beta}(r)}{dr} - \frac{2\pi}{|X_{\beta}(r)|^2} \frac{\partial |X_{\alpha}(r)|^2}{\partial \alpha} \Big|_{\alpha=\beta} \quad (14)$$

which can be written in a more compact form

$$\frac{\partial |X_{\alpha}(r)|^2}{\partial \alpha} \Big|_{\alpha=\beta} = -\frac{1}{2\pi} \frac{d}{dr} \left[|X_{\beta}(r)|^2 \frac{d\varphi_{\beta}(r)}{dr} \right]. \quad (15)$$

Note that (14) and (15) can be obtained by a direct differentiation of the fractional power spectrum or from the nonstationary Schrödinger equation for a harmonic oscillator, whose propagator is the fractional FT kernel. This result resembles the so-called transport-of-intensity equation, which deals with the Fresnel transformation [15]-[17]. This is not surprising, since both the fractional FT and the Fresnel transform belong to the class of canonical integral transforms, and the properties of any member of this class are related as well.

Although, in this paper we consider one-dimensional signals, the main results can be extended to the multi-dimensional case. In particular the application of the 2-D, anamorphic fractional FT allows one to obtain information about the partial derivatives of the phase. Thus, (15) can be generalized as

$$\frac{\partial |X_{\alpha_1,0}(r_1, r_2)|^2}{\partial \alpha_1} \Big|_{\alpha_1=\beta_1}$$

$$= -\frac{1}{2\pi} \frac{\partial}{\partial r_1} \left[|X_{\beta_1,0}(r_1, r_2)|^2 \frac{\partial \varphi_{\beta_1,0}(r_1, r_2)}{\partial r_1} \right]. \quad (16)$$

Below, we assume that at the fractional ($\beta = 0$)-domain, some *a priori* knowledge about the signal behavior is available. In particular, phase- and amplitude-modulated signals will be considered.

Case 1) Phase-Modulated Signal – Polynomial Phase Estimation: For phase-modulated signals $x(r) = A \exp[j\varphi(r)]$, where $|x(r)| = A$ is a constant, (14) reduces to

$$\frac{d^2 \varphi(r)}{dr^2} = -\frac{2\pi}{|A|^2} \frac{\partial |X_\alpha(r)|^2}{\partial \alpha} \Big|_{\alpha=0}, \quad (17)$$

and the n -th derivative of the phase for $n \geq 2$ can be written as

$$\frac{d^n \varphi(r)}{dr^n} = -\frac{2\pi}{|A|^2} \frac{\partial^{n-2}}{\partial r^{n-2}} \frac{\partial |X_\alpha(r)|^2}{\partial \alpha} \Big|_{\alpha=0} \quad (18)$$

In many applications, such as radar, sonar, and communications, polynomial phase signals

$$\varphi(r) = \sum_{n=0}^N a_n r^n, \quad (19)$$

with constant or slowly varying amplitude A are used as a model. Then, the angular derivative of the fractional FT spectra can also be represented as a polynomial function

$$\frac{\partial |X_\alpha(r)|^2}{\partial \alpha} \Big|_{\alpha=0} = -\frac{|A|^2}{2\pi} \sum_{n=2}^N n(n-1) a_n r^{n-2}. \quad (20)$$

In this case, the coefficients a_n for $n \geq 2$ can be found as the best fitting to the angular derivative of the fractional power spectrum or as

$$a_n = -\frac{1}{n!} \frac{2\pi}{|A|^2} \frac{\partial^{n-2}}{\partial r^{n-2}} \frac{\partial |X_\alpha(r)|^2}{\partial \alpha} \Big|_{\alpha=0, r=0}, \quad (21)$$

where the first method is more noise robust. This result can easily be checked for the quadratic chirp signal $x(t) = \exp(j\pi ct^2)$, for which the fractional power spectrum $|X_\alpha(r)|^2$ takes the form $|\cos \alpha + c \sin \alpha|^{-1}$, cf. [5]; note that $|X_\alpha(r)|^2$ is independent of r . Finally,

we obtain $\partial |X_\alpha(r)|^2 / \partial \alpha \Big|_{\alpha=0} = -c$, and thus, $a_2 = \pi c$.

Although this method does not permit to reconstruct the coefficients a_0 and a_1 in the decomposition (19), it can be useful for the estimation of the higher order coefficients because of its relative simplicity. Otherwise, the full algorithm, which is described in Sections III and IV, has to be applied.

Case 2) Phase-Modulated Signal – Edge Detection: The application of high-resolution phase spatial light modulators in optics, which permits the phase of the optical field $\varphi(\mathbf{r})$ to be proportional to an image $g(\mathbf{r})$, makes optical image processing more flexible. One of the important problems of image analysis is the localization of its edges. In spite of the fact that in digital image processing the diverse algorithms for edge detection are successfully implemented, not all of them are appropriated for optical image processing. Similar to the method proposed in [22], which is based on Fresnel diffraction, the positions of the edges can be found as the zero-crossings of the angular derivative of the fractional power spectrum. Indeed, for the 2-D, phase-modulated signal $f(\mathbf{r}) = A \exp[j\varphi(\mathbf{r})] = A \exp[jkg(\mathbf{r})]$, where k controls the depth of the phase modulation, (17) can be generalized as

$$\nabla^2 \varphi(\mathbf{r}) = k \nabla^2 g(\mathbf{r}) = -\frac{2\pi}{|A|^2} \frac{\partial |X_\alpha(\mathbf{r})|^2}{\partial \alpha} \Big|_{\alpha=0}, \quad (22)$$

where ∇^2 stands for the Laplacian operator. The zero-crossings of the fractional power spectra, $\partial |X_\alpha(\mathbf{r})|^2 / \partial \alpha \Big|_{\alpha=0} = 0$, thus correspond to the zero-crossings of $\nabla^2 g(\mathbf{r})$ and, therefore, determine the positions of the image edges.

Case 3) Amplitude-Modulated Signals – Extremum Point Detection: Let us consider a 2-D signal $x(\mathbf{r}) = A(\mathbf{r}) \exp(j2\pi \mathbf{k}\mathbf{r})$, where \mathbf{k} is a constant vector and $A(\mathbf{r}) > 0$. This type of signals in particular arises after propagation of a plane wave through an amplitude screen with transmittance function $A(\mathbf{r})$. In this case, it follows from (15) that the angular derivative of the fractional power spectrum is proportional to the positional derivative of the signal's in-

tensity

$$\left. \frac{\partial |X_{\alpha,0}(\mathbf{r})|^2}{\partial \alpha} \right|_{\alpha=0} = -k_1 \frac{d|A(\mathbf{r})|^2}{dr_1}, \quad (23)$$

and its zero-crossings thus correspond to the extremum points of $|A(\mathbf{r})|^2$ and $A(\mathbf{r})$. We believe that this relationship can be helpful for modeling of early vision systems where the scratch of the image, i.e., the maxima of $A(\mathbf{r})$, can be obtained from the knowledge of two close defocussed images associated with $|X_{\alpha_1, \alpha_2}(\mathbf{r})|^2$.

VI. DISCRETIZATION OF THE ALGORITHM

In this section, we will discuss the discrete version of the phase retrieval technique proposed in Section III. We suppose that two fractional power spectra $|X_{\beta-\alpha}(nT)|^2$ and $|X_{\beta+\alpha}(nT)|^2$ (corresponding to two Wigner distribution projections) at the close angles $\beta - \alpha$ and $\beta + \alpha$, where α is small (for example $\alpha \simeq 1^\circ$), are known for a set of equidistant sensor points. The fractional power spectra $|X_{\beta-\alpha}(nT)|^2$ and $|X_{\beta+\alpha}(nT)|^2$ can be obtained in several ways:

- i) measured in experiments (a simple optical setup for the measurements of the fractional power spectra was described in [24]);
- ii) calculated as the squared moduli of the corresponding fractional FT of $x(t)$;
- iii) calculated as the Radon transform of the Wigner distribution of $x(t)$ for two angles $\beta \pm \alpha$.

The discrete version of (9) for the estimation of the instantaneous frequency in the fractional β domain can then be written in the form

$$\begin{aligned} \hat{f}_\beta(nT) &= -\frac{1}{2\alpha} \frac{T}{2 |X_\beta(nT)|^2} \\ &= \left[|X_{\beta+\alpha}(nT)|^2 - |X_{\beta-\alpha}(nT)|^2 \right] *_n \text{sgn}(nT), \end{aligned} \quad (24)$$

where T is the discretization step, and $*_n$ denotes a discrete-time convolution. In order to avoid a separate estimation of $|X_\beta(nT)|^2$, the denominator $2|X_\beta(nT)|^2$ can, at least for small α , be approximated by $|X_{\beta+\alpha}(nT)|^2 + |X_{\beta-\alpha}(nT)|^2$.

The reconstructed signal at the fractional β domain can, up to the constant phase term, be found as

$$\begin{aligned} \hat{X}_\beta(nT) &= \\ |X_\beta(nT)| \exp \left[j \sum_{m=-M}^n 2\pi \hat{f}_\beta(mT)T \right], \end{aligned} \quad (25)$$

where N is chosen such that $f_\beta(nT) = 0$ for $n < -M$. In the case when two fractional FT spectra are taken around the angle $\beta = 0$, $\hat{X}_0(nT) = \hat{x}(nT)$ corresponds to the reconstructed version of the original signal. For $\beta \neq 0$, a subsequent discrete version of the fractional FT for the angle $-\beta$ has to be applied to $\hat{X}_\beta(nT)$ in order to reconstruct the original signal. Several algorithms for calculation of the fractional FT have been proposed in [25]-[27].

In what follows, we will illustrate in several numerical examples how the signal, up to a constant phase term, can be reconstructed from two close fractional power spectra only, i.e., from two Wigner distribution projections. In order to emphasize the quality of the reconstruction, we will also show the *pseudo* Wigner distribution of the original and the reconstructed signal. The *pseudo* Wigner distribution is calculated according to its definition

$$\begin{aligned} W_{\hat{x}}(n, k) &= 2T \sum_{m=-N}^{N-1} \hat{x}[(n+m)T] \hat{x}^*[(n-m)T] \\ &\quad \times w(mT) \exp(-j2\pi mk/N), \end{aligned} \quad (26)$$

where $w(nT)$ is an appropriately chosen window function, and the value of N is chosen such that $\hat{x}(nT) \simeq 0$ for $|n| \geq N$.

Note that by choosing an appropriate window function, the signal reconstruction can also be achieved from two close projections of the *pseudo* Wigner distribution as long as the angle β is small; see Section III.

VII. EXAMPLES

In this section we demonstrate the efficiency of the proposed algorithm on various examples.

Example 1- Monocomponent Signal With Monotonic Instantaneous Frequency: We start with the reconstruction of a monocomponent

signal, whose instantaneous frequency is a monotonic function. A signal of the form

$$x(t) = e^{-(2.25t)^8} \times e^{j \int_{-\infty}^t [360 \arctan(20t) + 256\pi] dt} \quad (27)$$

is considered inside the time interval $|t| \leq 1/2$, with $T = 1/1024$. Its *pseudo* Wigner distribution is calculated, by using a Hanning window $w(t)$ having a width $T_w = 1/8$. After the Wigner distribution has been obtained, we assume that only two of its projections, for angles $\alpha = -1^\circ$ and $\alpha = 1^\circ$, sampled at $2N = 1024$ points are known. Note that these two fractional power spectra $|X_\alpha(nT)|^2$ and $|X_{-\alpha}(nT)|^2$ ($\alpha = 1^\circ$), can be measured in an optical system. In our case, these two projections are simulated by using the MATLAB Radon function, taking the pseudo Wigner distribution matrix as the argument. The described procedure [cf. (24)] is then used for the reconstruction of the signal's instantaneous frequency, its phase, and the signal itself [(25)], from these two projections only.

The original *pseudo* Wigner distribution is given in Fig. 1(a). Its Radon-Wigner transform $|X_\alpha(nT)|^2$ for angles $\alpha \in [0^\circ, 180^\circ]$ [cf. (3)] is presented in Fig. 1(b). The difference of the two projections, $(|X_\alpha(nT)|^2 - |X_{-\alpha}(nT)|^2)/2\alpha$ for $\alpha = 1^\circ$ is shown in Fig. 1(c). The reconstructed instantaneous frequency and the reconstructed phase are given in Fig. 1(d) and (e), respectively, by a dash-dot line, whereas the original, exact values are represented by solid lines. We can see that the agreement between the reconstructed and the original instantaneous frequency is very high. The phase has a constant shift, as expected. In order to demonstrate the quality of the signal reconstruction, the reconstructed *pseudo* Wigner distribution calculated according to (26) is given in Fig. 1(f).

Example 2 – Monocomponent Signal With Nonmonotonic Instantaneous Frequency: Next, we consider a signal with a nonmonotonic instantaneous frequency

$$x(t) = e^{-(2.25t)^8} \{1 - e^{-(20t)^{20}}\} e^{j \int_{-\infty}^t \omega_i(t) dt}$$

$$\omega_i(t) = 256\pi + 128\pi \operatorname{sgn}(\cos(8\pi t + \pi/4))$$

$$\times \sqrt{|\cos(8\pi t + \pi/4)|}. \quad (28)$$

The peculiarity of this signal is that it has a region with almost zero amplitude. The discretization parameters are the same as in Example 1. Fig. 2 shows the original *pseudo* Wigner distribution, its Radon transform, the difference of two projections, and the reconstructed instantaneous frequency, phase, and *pseudo* Wigner distribution. As in the previous example, a high-quality reconstruction of the instantaneous frequency and phase, outside the zero amplitude region, is observed. Certainly, the phase reconstruction inside the region of zero amplitude has no sense. Since this signal can be considered as the concatenation of two different parts, the reconstructed phase of both parts is in good agreement with the original one, up to different constant terms.

Example 3 – Multicomponent Signal: The reconstruction of a multicomponent signal,

$$x(t) = e^{-(2.25t)^8} \times \{e^{j \int_{-\infty}^t \omega_1(t) dt} + 0.5e^{j \int_{-\infty}^t \omega_2(t) dt}\}$$

$$\omega_1(t) = 128\pi \sin(4t\pi) + 256\pi$$

$$\omega_2(t) = 512\pi |t| + 128\pi, \quad (29)$$

is considered in this example. Note that the instantaneous frequency of this signal shows a rather complex form. Nevertheless, for this multicomponent signal we are still able to obtain a satisfactory reconstruction of the phase and the *pseudo* Wigner distribution, using only two close fractional power spectra (see Fig. 3). The discretization parameters are the same as in Example 1 ($\beta = 0$, $\alpha = 1^\circ$).

Example 4 – Reconstruction of a Monocomponent Signal From Projections Around a Nonzero Angle: In this example, we consider the reconstruction of a signal that is similar to that in Example 1

$$x(t) = e^{-(3.5t)^8} \times e^{j \int_{-\infty}^t 15\pi \sinh^{-1}(100t) dt} \quad (30)$$

but from two close projections around the angle where the instantaneous power of the signal changes significantly. Now we use a wide

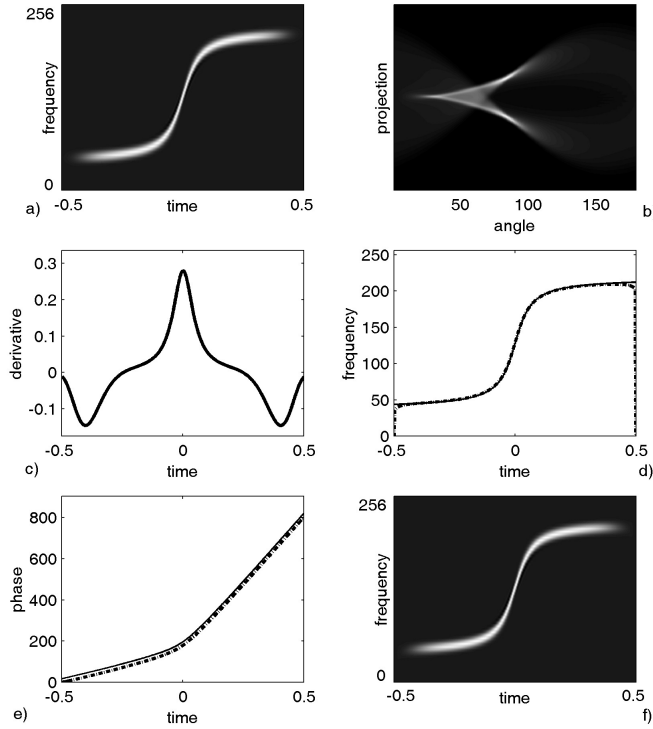


Fig. 1. Monocomponent signal with monotonic instantaneous frequency and its reconstruction from two close fractional power spectra. (a) Original *pseudo* Wigner distribution. (b) Projections of the *pseudo* Wigner distribution (Radon-Wigner transform). (c) Derivative approximation: difference of two close projections calculated at 1° and -1° , and divided by the angle step. (d) Reconstructed (dash-dot) and original (solid line) instantaneous frequency of the signal. (e) Reconstructed (dash-dot) and original (solid line) phase of the signal. (f) Reconstructed *pseudo* Wigner distribution.

lag window function, extending over the entire considered time interval $T_w = 1$, corresponding to $2N = 256$ points. This window produces a distribution which is close to the pure Wigner distribution, without the attribute *pseudo*. The signal discretization parameters and the window size in this example are such that the number of points along the time and the frequency axes is the same; i.e., the Wigner distribution in discrete form is a square matrix. We now reconstruct the signal in the fractional domain for the angle $\beta = -45^\circ$, with $\alpha = 1^\circ$, which implies that the reconstructed signal is the fractional Fourier transform of the original signal for $\beta = -45^\circ$. The original signal can easily be obtained as an inverse fractional FT for the same angle. Comparing Fig. 4(a) and (d), one can observe

a high quality of the signal reconstruction. Indeed, Fig. 4(d) is the rotated version of the WD reconstructed from two close projections around the angle $\beta = -45^\circ$.

Example 5 – Influence of the Angle Difference on the Reconstruction Quality: The signal from the previous example is used for the numerical illustration of the influence of angle difference α in (24). The reconstructions are performed from the projections around $\beta = 0^\circ$ for three values of α : $\alpha = 1^\circ$, $\alpha = 10^\circ$, and $\alpha = 20^\circ$ (see Fig. 5). We can see that near the end points, a deviation in the reconstructed distribution and the instantaneous frequency exists for $\alpha = 10^\circ$ and that this deviation is very emphatic for $\alpha = 20^\circ$. The accuracy of reconstruction also depends on the complexity of the fractional amplitude $|X_{\beta \pm \alpha}(nT)|^2$ in

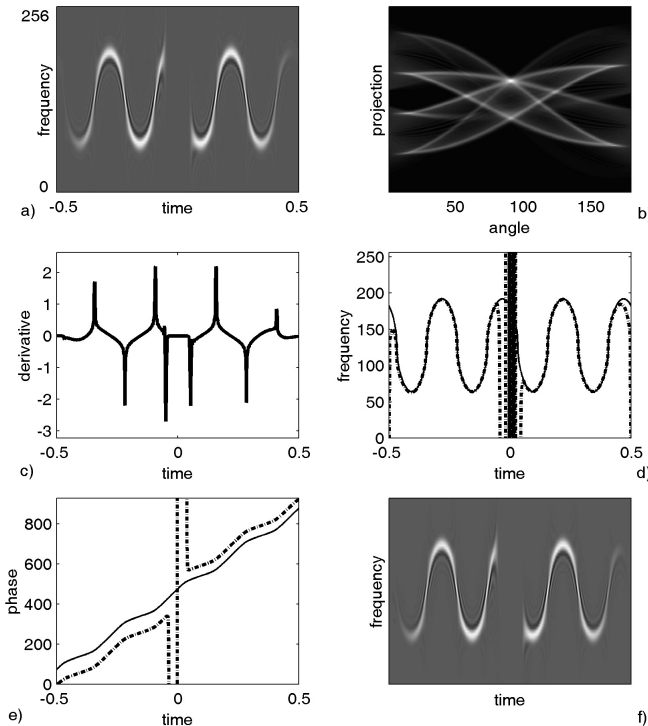


Fig. 2. Monocomponent signal with nonmonotonic instantaneous frequency and zero-amplitude in its central part and its reconstruction from two close fractional power spectra. (a) Original *pseudo* Wigner distribution. (b) Projections of the *pseudo* Wigner distribution (Radon-Wigner transform). (c) Derivative approximation: difference of two close projections calculated at 1° and -1° and divided by the angle step. (d) Reconstructed (dash-dot) and original (solid line) instantaneous frequency of the signal. (e) Reconstructed phase of the signal. (f) Reconstructed *pseudo* Wigner distribution.

(24). From this illustration, and other similar numerical experiments with various signals, we have concluded that the values of α in the order of 1° , up to few degrees, produce satisfactory numerical results.

Example 6 – Noisy Signal: The reconstruction algorithm is tested for noisy cases as well. The signal from Example 1, contaminated by Gaussian, complex-valued, white noise $\nu(t)$

$$x(t) = \exp[-(2.25t)^8] \times \{Ae^{j \int_{-\infty}^t [360 \arctan(20t) + 256\pi] dt} + \nu(t)\}, \quad (31)$$

is considered. Various values of the local SNR $= 20 \log(A/\sigma_\nu)$ have been used in simulations. Fig. 6 presents the reconstruction result for a SNR=10 dB. Small deviations of the reconstructed distribution can be seen in this case. From numerous calculations, we have

concluded that the reconstruction threshold is at about SNR = 3 dB. Below this value, the degradation of the reconstructed distribution is significant. Nevertheless, it seems that for signal reconstruction in a very high noise, the knowledge of several pairs of close projections would improve the results. In that case we can calculate the differences of the fractional power spectra for several small angles and then average them. Furthermore, using other discrete differentiators that are different from the simple one given by a mere difference would also improve noisy case results. However, since the original algorithm produces a satisfactory reconstruction, even for as low a SNR as a few decibels, we have not implemented this variation of the algorithm, for now.

Note that the original noisy distribution,

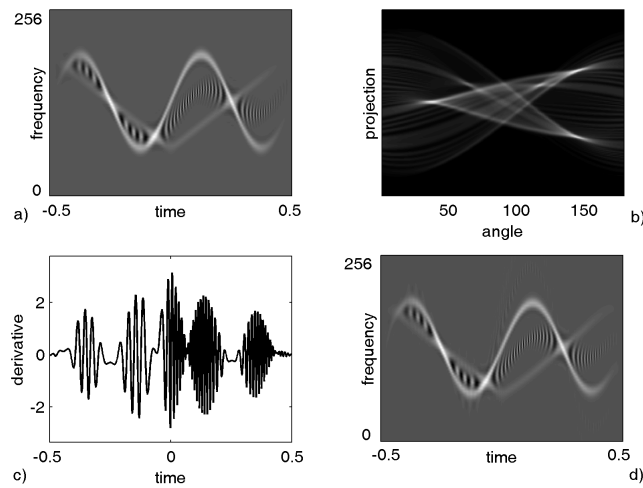


Fig. 3. Multicomponent signal and its reconstruction from two close fractional power spectra. (a) Original *pseudo* Wigner distribution. (b) Projections of the *pseudo* Wigner distribution (Radon-Wigner transform). (c) Derivative approximation: difference of two close projections calculated at 1° and -1° and divided by the angle step. (d) Reconstructed *pseudo* Wigner distribution.

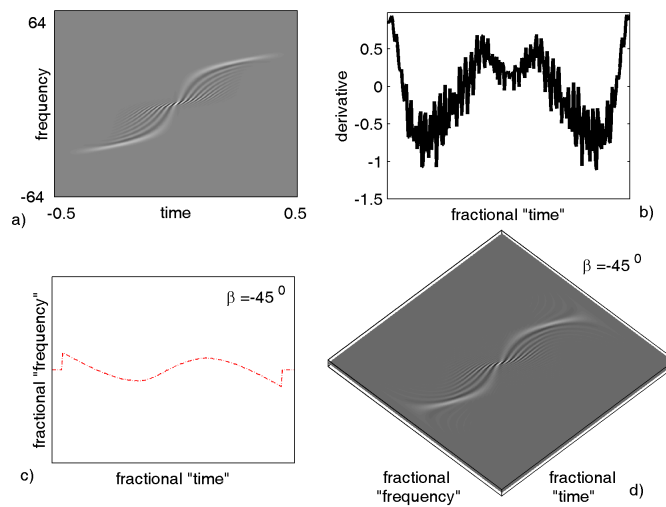


Fig. 4. Monocomponent signal with monotonic instantaneous frequency and its reconstruction from two close fractional power spectra around the angle $\beta = -45^\circ$. (a) Original Wigner distribution. (b) Derivative approximation: difference of two close projections calculated at 1° and -1° and divided by the angle step. (c) Reconstructed instantaneous frequency of the signal. (f) Reconstructed Wigner distribution.

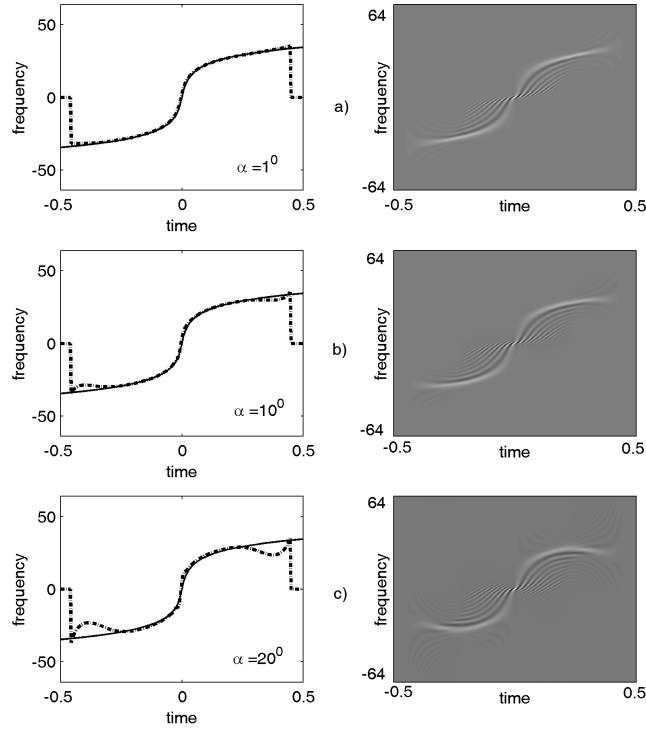


Fig. 5. Monocomponent signal with monotonic instantaneous frequency and its reconstruction from two close fractional power spectra for various angle differences in the derivative approximation. Reconstructed instantaneous frequency and reconstructed Wigner distribution for (a) $\alpha = 1^\circ$. (b) $\alpha = 10^\circ$. (c) $\alpha = 20^\circ$.

Fig. 6(a), and the reconstructed distribution, Fig. 6(f) differ slightly. The noise in the original distribution is additive, whereas the reconstructed distribution is obtained from the estimated noisy instantaneous frequency and reconstructed noisy amplitude. Due to extremely fast variations of the noise, some mismatching between the variations in the amplitude and the instantaneous frequency can exist, and cause slightly different behavior of these distributions. It is exhibited more and more for lower SNR values, and below about 3 dB, the algorithm stops to produce satisfactory results.

VIII. CONCLUSIONS

In this paper, we have established the relation between the angular derivative of the fractional power spectra and the instantaneous frequency, and we have proposed a method of phase reconstruction from only two close pro-

jections of the Wigner distribution. The numerical simulations show that the discussed phase retrieval algorithm produces good results for several types of signals. The reconstruction technique works well for a signal-to-noise ratio as low as about 3 dB. The main advantages of the proposed method are that it is noniterative and demands a minimum number of initial data – only two close fractional FT power spectra – which are related to easily measurable power distributions. In optics and quantum mechanics, for instance, the fractional FT spectrum corresponds to the intensity distribution and the probability distribution, respectively.

We have also briefly discussed the possible applications of the angular derivatives of the fractional FT power spectra for signal processing, time-varying filtering, edge detection, etc. It becomes especially attractive if only the fractional spectra of a signal are known.

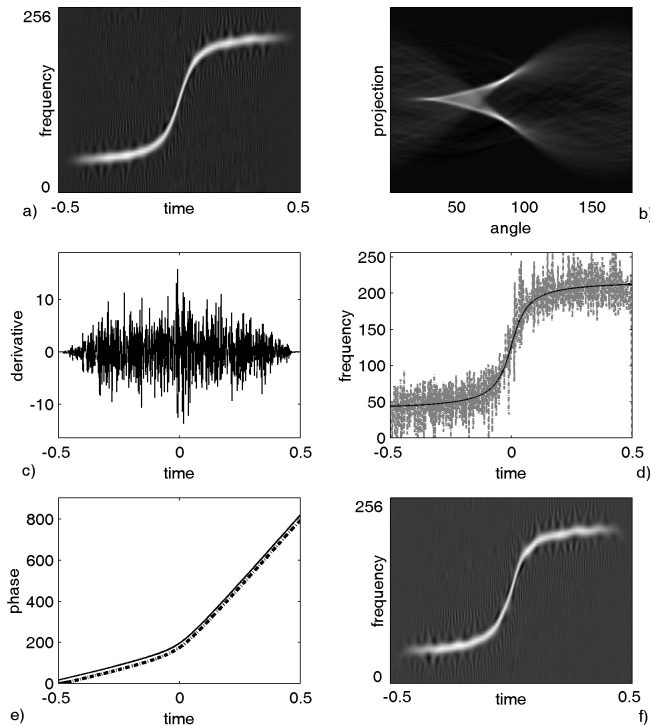


Fig. 6. Noisy signal (SNR = 10 dB) and its reconstruction from two close fractional power spectra. (a) Original Wigner distribution. (b) Projections of the Wigner distribution (Radon-Wigner transform). (c) Derivative approximation: difference of two close projections calculated at 1° and -1° , and divided by the angle step. (d) Reconstructed (dash-dot) and original (solid line) instantaneous frequency of the signal. (e) Reconstructed (dash-dot) and original (solid line) phase of the signal. (f) Reconstructed Wigner distribution.

REFERENCES

- [1] Z. Zalevsky, D. Mendlovic, and R. G. Dorsch, "Gerchberg-Saxton algorithm applied in the fractional Fourier or the Fresnel domain," *Opt. Lett.*, vol. **21**, pp. 842-844, 1996.
- [2] H. M. Ozaktas, Z. Zalevsky, and M. A. Kutay, *The Fractional Fourier Transform*, Wiley, 2001.
- [3] W. X. Cong, N. X. Chen, and B. Y. Gu, "Recursive algorithm for phase retrieval in the fractional Fourier-transform domain," *Appl. Opt.*, vol. **37**, pp. 6906-6910, 1998.
- [4] W. X. Cong, N. X. Chen, and B. Y. Gu, "Phase retrieval in the Fresnel transform system - a recursive algorithm," *J. Opt. Soc. Am. A*, vol. **16**, pp. 1827-1830, 1999.
- [5] L. B. Almeida, "The fractional Fourier transform and time-frequency representations," *IEEE Trans. Signal Process.*, vol. **42**, pp. 3084-3091, 1994.
- [6] M. G. Raymer, M. Beck, and D. F. McAlister, "Complex wave-field reconstruction using phase-space tomography," *Phys. Rev. Lett.*, vol. **72**, pp. 1137-1140, 1994.
- [7] J. Tu and S. Tamura, "Analytic relation for recovering the mutual intensity by means of intensity information," *J. Opt. Soc. Am. A*, vol. **15**, pp. 202-206, 1998.
- [8] H. M. Ozaktas, N. Erkaya, and M. A. Kutay, "Effect of fractional Fourier transformation on time-frequency distributions belonging to the Cohen class," *IEEE Signal Process. Lett.*, vol. **3**, pp. 40-41, 1996.
- [9] X.-G. Xia, Y. Owechko, B. H. Soffer, and R. M. Matic, "Generalized-marginal time-frequency distributions," *Proc. IEEE-SP International Symposium on Time-Frequency and Time-Scale Analysis*, pp. 509-512, 1996.
- [10] O. Akay and G. F. Boudreaux-Bartels, "Joint fractional representations," *Proc. IEEE-SP International Symposium on Time-Frequency and Time-Scale Analysis*, pp. 417-420, 1998.
- [11] B. Ristic and B. Boashash, "Kernel design for time-frequency signal analysis using the Radon transform," *IEEE Trans. Signal Process.*, vol. **41**, pp. 1996-2008, 1993.
- [12] J. C. Wood and D. T. Barry, "Tomographic time-frequency analysis and its application toward time-varying filtering and adaptive kernel design for multicomponent linear-FM signals," *IEEE Trans. Signal Process.*, vol. **42**, pp. 2094-

- 2104, 1994.
- [13] J. C. Wood and D. T. Barry, "Radon transformation of time-frequency distributions for analysis of multicomponent signals," *IEEE Trans. Signal Process.*, vol. **42**, pp. 3166-3177, 1994.
- [14] A. W. Lohmann and B. H. Soffer, "Relationships between the Radon-Wigner and fractional Fourier transforms," *J. Opt. Soc. Am. A*, vol. **11**, pp. 1798-1801, 1994.
- [15] M. R. Teague, "Deterministic phase retrieval: a Green function solution," *J. Opt. Soc. Am.*, vol. **73**, pp. 1434-1441, 1983.
- [16] N. Streibl, "Phase imaging by the transport equation of intensity," *Opt. Commun.*, vol. **49**, pp. 6-10, 1984.
- [17] K. Ichikawa, A. W. Lohmann, and M. Takeda, "Phase retrieval based on the Fourier transport method: experiments," *Appl. Opt.*, vol. **27**, pp. 3433-3436, 1988.
- [18] T. E. Gureev, A. Roberts, and K. A. Nugent, "Partially coherent fields, the transport-of-intensity equation, and phase uniqueness," *J. Opt. Soc. Am. A*, vol. **12**, pp. 1942-1946, 1995.
- [19] F. Boudreaux-Bartels, "Mixed time-frequency signal transformations," in *The Transforms and Applications Handbook*, ed. A. D. Poularikas, CRC Press, Alabama, pp. 887-962, 1996.
- [20] T. Alieva and M. J. Bastiaans, "On fractional Fourier transform moments," *IEEE Signal Process. Lett.*, vol. **7**, pp. 320-323, 2000.
- [21] T. Alieva, M. J. Bastiaans and L.J. Stanković, "Wigner distribution reconstruction from two projections," in *Proceeding of the IEEE Workshop on Statistical Signal Processing*, Singapore, pp.325-328, 6-8th August 2001.
- [22] M.A. Vorontsov, "Parallel image processing based on an evolution equation with anisotropic gain: integrated optoelectronic architectures," *J. Opt. Soc. Am. A*, vol. **16**, pp. 1623-1637, 1999.
- [23] A. Kutay, H. M. Ozaktas, O. Ankan, and L. Onural, "Optimal filtering in fractional Fourier domains," *IEEE Trans. Signal Process.*, vol. **45**, pp. 1129-1143, 1997.
- [24] A. W. Lohmann, "Image rotation, Wigner rotation, and the fractional Fourier transform," *J. Opt. Soc. Am. A*, vol. **10**, pp. 2181-2186, 1993.
- [25] H. M. Ozaktas, O. Ankan, M. A. Kutay, and G. Bozdagi, "Digital computation of the fractional Fourier transform," *IEEE Trans. Signal Process.*, vol. **44**, pp. 2141 -2150, 1996.
- [26] S. C. Pei, M. H. Yeh, and C. C. Tseng, "Discrete fractional Fourier transform based on orthogonal projections," *IEEE Trans. Signal Process.*, vol. **47**, pp. 1335 -1348, 1999.
- [27] C. Candan, M. A. Kutay, and H. M. Ozaktas, "The discrete fractional Fourier transform," *IEEE Trans. Signal Process.*, vol. **48**, pp. 1329 -1337, 2000.